Constructive Use of GNSS NLOS-Multipath: Augmenting the Navigation Kalman Filter with a 3D Model of the Environment

Aude Bourdeau
ISAE/TeSA
University of Toulouse, France

Mohamed Sahmoudi
ISAE/TeSA
University of Toulouse, France

Jean-Yves Tourneret
IRIT/ENSEEIHT/TeSA
University of Toulouse, France

***Abstract*—In this paper, we introduce a GNSS positioning approach that uses constructively non-line-of-sight (NLOS) signals. A 3D model of the environment is used to predict the geometric paths of NLOS signals. More precisely, we propose a version of the extended Kalman filter augmented by a 3D model, referred to as 3D AEKF, for GNSS navigation in NLOS context. In the proposed approach, the measurement model traditionally based on the trilateration equations is constructed from the received paths estimated by the 3D model. The Jacobian of the measurement model is calculated through knowledge of the wall on which the reflection has occured. To use even less reliable measurements, a robust version of the 3D AEKF is also proposed. Simulations conducted in different realistic configurations allow the performance of the proposed method to be evaluated.**

I. Introduction

The number of global navigation satellite system (GNSS) applications has steadily increased over the last decade, in particular for personal mobility (e.g., GNSS-enabled mobile phones, smartphones and services). Intelligent systems for road transport is also an important segment of the GNSS market including in-car navigation and road user charging. However, the urban environment presents significant challenges for satellite positioning. On the one hand, the user is expecting for a positioning accuracy greater than that obtained in open sky areas, because of the proximity of the various points of interest and intersections. On the other hand, the urban environment creates difficulties in the GNSS signal reception, particularly because of satellite masking and multipath phenomena. As a consequence, the receiver delivers a position that can be biased by an error of several tens of meters [1], [2], when it is not totally impossible to calculate a position. This is particularly true in the context of urban canyons, i.e., when the streets are very narrow and/or the buildings are very high.

The main undesirable phenomena encountered in urban areas are attenuations, multipath and shadowing effects. Multipath propagation occurs when GNSS signals bounce off buildings and reach the receiver's antenna via different paths with a traveling time longer than that of the line-of-sight (LOS) path. Multipath signals can be very strong and have small relative delays which makes them difficult to be distinguished from the desired path signal. Examples of efficient in-receiver multipath mitigation methods include the narrow correlator, the strobe correlator, the multipath estimating delay lock loop, the multipath elimination technology, the vision correlator and the fast iterative maximum-Likelihood algorithm [1], [3]–[5]. However, in urban canyon environment, the number of LOS satellites is very low and the position dilution of precision (DOP) of these satellites is usually unsatisfactory. We suggest in this work to investigate the constructive use of multipath signals instead of simply mitigating those reflections as in most current GNSS receivers. If the user is in a non-line-of-sight (NLOS) context, the receiver will consider the received GNSS signal as a LOS and will estimate a pseudorange from the satellite biased by several tens of meters. It has been recognized that a stand-alone GNSS receiver is not enough to provide reliable location service in severely obstructed signal conditions. To deal with these difficulties, the GNSS receiver can be assisted by several sources of information such as inertial navigation sensors, wireless network or vision, requiring additional infrastructure and complexe hybridation technologies. Another possibility is to exploit all the available information for improving the positioning performance in these kind of harsh environments. One way consists of comparing visible satellites with an a priori knowledge of the shadowed satellites [6]. Another way is to be able to use NLOS constructively rather than just deleting them. However, the difficulty to use NLOS multipath is in the capability to model the lengths of these indirect paths. Without this knowledge, it is difficult to correct the distance error carried by the signal that has undergone multipath. In [7] a geometric path model is used, whose parameters are estimated by a nonlinear filter. In [8] and [9], paths are calculated by laser scanning of the environment.

In this paper, we propose a new navigation strategy based on a 3D model of the environment. This 3D tool is based on a ray tracing algorithm predicting the signal reception of systems such as GPS and GALILEO integrated into 3D virtual scenes of known urban areas. The ray tracing algorithm computes the shadowing effects and the multipaths generated by the objects of a given geometrically represented environment [10]. For reason of simplicity (in this preliminary contribution), we use a simplified 3D model and we consider that the NLOS-multipath has only one reflection path. This assumption is coherent with the results presented in [2] which show that multipath with only one reflection are generally the most powerful.

We introduce a new approach of position computation with indirect path measurements by tightly integrating the 3D model information in an extended Kalman filter (EKF). In the proposed method, the measurement model traditionally based on the trilateration equations is constructed from the received paths estimated by the 3D model. The Jacobian of the resulting measurement model is calculated through knowledge of the wall on which the received signal has been reflected. To use even less reliable measurements, a robust version of the proposed filter based on ideas developped in [11] is also proposed.

II. Navigation Filter Augmented by a 3D Model

The Kalman filter is one of the most popular and widely used implementations in navigation for multi-sensor data fusion. In a Bayesian framework, the receiver position is determined by an estimator that minimizes the mean square error between the state vector and its estimator under the assumptions of linear state and measurement equations. When the state and/or measurement equations are nonlinear, the minimum mean square error (MMSE) estimator can be approximated by the EKF that has received a considerable attention for navigation applications. This paper concentrates on the EKF-based MMSE estimator (possibly robustified using M-estimation techniques) even if other solutions (increasing computational complexity) such as particle filters could also be investigated [12].

A. EKF principles for GNSS navigation

The receiver clock bias is a time-varying error that affects simultaneously all range measurements in the same fashion. Clock bias prediction is feasible today by integrating a chip-scale atomic clock (CSAC) in a GNSS receiver [13]. Due to the high degree of CSAC frequency stability, the clock bias is predictable, and thus only three satellites are needed for a full navigation solution. To focus on the integration aspect with parameters associated with user environment, we do not consider the clock bias estimation issue in this paper since we use only simulated GPS signals and a 3D urban model.

The state model used for GNSS is based on the dynamic equations associated with the vehicle motion. We use a model with constant speed and we assume that the clock bias of the receiver is known (thus the clock bias is not included in the state vector). When the receiver has a uniform motion (i.e., with near constant velocity), the navigation performance is improved by including the velocity states in the dynamic model. In this case, velocity is modeled as a random-walk process and position is modeled as the integral of velocity via the following state transition equation

$$X_k = \Phi X_{k-1} + v_k$$

with X_k defined as

$$X_k = [x_k \ y_k \ z_k \ \dot{x_k} \ \dot{y_k} \ \dot{z_k}]^T$$

where $(x_k \ y_k \ z_k)$ and $(\dot{x_k} \ \dot{y_k} \ \dot{z_k})$ are the three receiver position and velocity components, and ^{T} denotes transposition.

The state transition matrix Φ is defined as

$$\Phi = \begin{bmatrix} 1 & 0 & 0 & \Delta t & 0 & 0 \\ 0 & 1 & 0 & 0 & \Delta t & 0 \\ 0 & 0 & 1 & 0 & 0 & \Delta t \\ 0 & 0 & 0 & 1 & 0 & 0 \\ 0 & 0 & 0 & 0 & 1 & 0 \\ 0 & 0 & 0 & 0 & 0 & 1 \end{bmatrix},$$

and $v_k \sim \mathcal{N}(0, Q)$ is the process noise assumed to be white Gaussian with covariance matrix Q. Δt is the time step between two iterations.

The measurement vector Y_k consists of the pseudoranges ρ_k^i, for $i = 1, \ldots, n$ (where n is the number of in view satellites) resulting from the visible satellites at time instant k, i.e.,

$$Y_k = [\rho_k^1 \cdots \rho_k^n]^T$$
$$\rho_k^i = \|X_{\text{sat}}^{i,k} - X_{\text{rec}}^k\| + w_k$$

where $X_{\text{sat}}^{i,k}$ is the vector of coordinates for the i^{th} observed satellite at time instant k and X_{rec}^k contains the receiver coordinates. In outdoor environments, the measurement noise $w_k \sim \mathcal{N}(0, R)$ is usually modeled as a white Gaussian sequence independent from v_k, with covariance matrix R.

When the navigation filter has to be constructed with the satellite pseudoranges, the nonlinearity of the measurement model requires the use of an EKF. Fig. 1 shows the principle

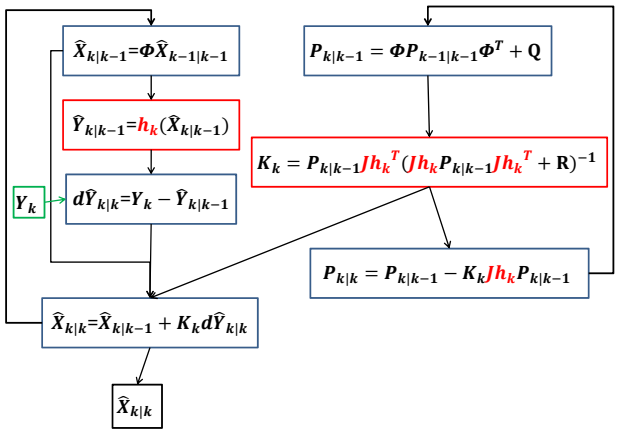

Fig. 1. Extended Kalman Filter

of an EKF dedicated to satellite navigation. In this figure, $\hat{X}_{k|k}$ is the estimated state vector at time instant k using the measurements up to time k and $P_{k|k}$ is the covariance matrix of $\hat{X}_{k|k}$. Moreover, h_k and Jh_k denote the nonlinear function of the measurement model and its Jacobian, respectively.

In what we call thereafter the classical version of the navigation filter, the trilateration equations and their derivatives are used for h_k and Jh_k, i.e.,

$$h_k^i(\hat{X}_{k|k-1}) = \hat{\rho}_{k|k-1}^i = \|X_{\text{sat}}^{i,k} - \hat{X}_{\text{rec}}^{k|k-1}\|. \quad (1)$$

The trilateration equations provide a good measurement model when the signal is received in LOS conditions. They represent

the geometric distance between the satellites and the receiver. However, if the signal is received after reflection (due to multipath), this model no longer corresponds to the geometrical reality. Consequently, the predicted measurements will differ from the actual measurements, and the Jacobian will not be correct to calculate the update. In this situation, we propose to use a 3D city model to determine the true geometric path travelled by the signal. Note that the navigation filter using the 3D city model will be referred to as 3D augmented navigation filter (3D ANF).

B. Integration of a 3D Model in an EKF

In the simple case of a single reflection, the geometric distance between the i^{th} satellite and the receiver can be decomposed into two segments. Consequently, (1) has to be replaced by

$$\hat{\rho}^i_{k|k-1} = \|X^i_{\text{sat},k} - I^i_k\| + \|I^i_k - \hat{X}^{k|k-1}_{\text{rec}}\| \tag{2}$$

where I^i_k is the reflection point for the signal resulting from the i^{th} satellite at time k. Note that I^i_k depends on the satellite position, the equation of the reflector wall and especially the receiver postion i.e., $\hat{X}_{k|k-1}$. Consequently, to know the correct Jacobian, we have to express I^i_k as a function of $\hat{X}_{k|k-1}$ in order to derive this expression.
Thanks to the ephemeris, we can compute the satellite positions at the time of emission. Thus, the only unknown invariant in (2) is the equation of the reflector wall. The 3D city model can provide us with this information. For a given position of the receiver and the corresponding satellite positions, this tool is able to estimate the received NLOS signals and the walls on which these signals have been backscattered.

C. Geometric Modeling of NLOS point of reflection

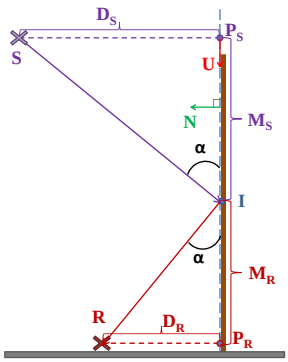

Fig. 2. Geometric path of a signal reflected on a wall (S is the satellite and R is the receiver).

For simplification purpose, we adopt temporarily the notation of Fig. 2, where S and R are the satellite and receveir positions and I is the reflection point. The wall is defined by its normal vector $\mathbf{N}$ and the coefficient d, through the equation

$$N_x X + N_y Y + N_z Z + d = 0.$$

$\mathbf{N}$ and d can be determined thanks to the 3D city model. The projections of S and R on the wall, denoted as P_S and P_R, are calculated as

$$\begin{cases} S - D_S\mathbf{N} = P_S \\ \mathbf{N^T}P_S + d = 0 \end{cases} \Rightarrow D_S = \frac{d + \mathbf{N^T}S}{\mathbf{N^T}\mathbf{N}}$$

$$\begin{cases} R - D_R\mathbf{N} = P_R \\ \mathbf{N^T}P_R + d = 0 \end{cases} \Rightarrow D_R = \frac{d + \mathbf{N^T}R}{\mathbf{N^T}\mathbf{N}}.$$

From P_S and P_R, we can define the unit direction vector $\mathbf{U}$ of the line connecting these two points

$$\mathbf{U} = \frac{P_R - P_S}{\|P_R - P_S\|}.$$

The laws of geometrical optics indicate that the angles $\widehat{P_S I S}$ and $\widehat{P_R I R}$ have the same value α. Since M_S (resp. M_R) is the distance between P_S and I (resp. P_R and I), the following results can be obtained

$$\tan\alpha = \frac{|D_S|}{M_S} = \frac{|D_R|}{M_R} \Rightarrow M_S = \frac{M_R\,|D_S|}{|D_R|}$$

$$M_S + M_R = \|P_R - P_S\| \Rightarrow M_R = \|P_R - P_S\| - M_S$$

hence

$$M_S = \frac{\|P_R - P_S\|}{\frac{|D_S|}{|D_R|} + 1}.$$

Finally, I is given by

$$I = P_S + M_S\mathbf{U}.$$

By replacing each element with its expression in terms of R, S, $\mathbf{N}$ and d, we obtain an equation for I that can be differentiated with respect to each component of R. In other words, we can differenciate (2) with respect to $\hat{X}_{k|k-1}$.

D. Robust Kalman for improved performance

When the 3D model is used as the measurement model, a new problem appears. The 3D model is able to give geometric information only for the paths associated with signals that are visible to him at the position examined. This means that if some signals received by the receiver are not visible according to the model, the information they provide cannot be used. Indeed, without the ability to predict measurements $\hat{\rho}^i_{k|k-1}$ for these signals, it is not possible to calculate their corresponding residuals $d\hat{Y}^i_{k|k}$. This problem appears in particular when the predicted position is inside a building. If the trajectory is close to a wall, this situation can easily occur, even without having a large prediction error. In this case, the 3D model cannot predict any measurement since it considers that no satellite is visible.
To use the information obtained for signals that are not seen by the 3D model, one solution is to use temporarily a less accurate but available model defined by the trilateration equations. However, the use of these equations should be done carefully. If the received signal is actually a multipath, the filter is biased because of the modeling error resulting from the trilateration,

and a more accurate solution computed by the 3D ANF may be corrupted. To avoid such cases, we propose to use a robust version of the EKF that mitigates the modeling errors due to trilateration.

Global robustness can be added in the Kalman filter by an adaptive stochastic method using a robust M-estimation approach [11]. This method uses a weighting function to adapt and correct the contribution of the updated parameters in the Kalman filter. Instead of minimizing the sum of residual squares $\left(d\hat{Y}^i_{k|k}\right)^2$, the M-estimation method minimizes a so-called influence function defined as [14]

$$\psi(d\hat{Y}) = \begin{cases} d\hat{Y} & \text{if} \quad |d\hat{Y}| < a \\ a & \text{if} \quad a \leq |d\hat{Y}| < c \\ (a/c)d\hat{Y}\exp\left(1 - d\hat{Y}^2/c^2\right) & \text{if} \quad |d\hat{Y}| \geq c \end{cases}$$

The associated diagonal weight matrix is defined by

$$D(d\hat{Y}) = \begin{cases} 1 & \text{if} \quad |d\hat{Y}| < a \\ a/|d\hat{Y}| & \text{if} \quad a \leq |d\hat{Y}| < c \\ (a/c)\exp\left(1 - d\hat{Y}^2/c^2\right) & \text{if} \quad |d\hat{Y}| \geq c \end{cases}$$

The robust EKF equations are identical to those of the EKF except for the innovation step, where the residuals are weighted by the matrix D

$$V_k = D\left(Y_k - \hat{Y}_{k|k-1}\right).$$

Since the residuals with low weights have reduced reliability, the robust processing associates a higher value to their estimated noise. A heuristic approach is followed here to choose the inverse of D for weighting R. Consequently, the Kalman gain matrix for the robust version can be calculated as

$$K_k = P_{k|k-1}Jh_k^T\left(Jh_kP_{k|k-1}Jh_k^T + D^{-1}R(D^{-1})^T\right)^{-1}.$$

The parameters a and c are chosen to keep good measurements and in the same time eliminate efficiently the outliers. Constant parameters did not yield good results because of the constraint environment. In other words, there are situations where there are two few received signals to compute an accurate position. If this situation lasts too long, the estimated position may have drifted significantly from the actual position when new signals become available. Without taking this situation into account, the robust EKF will reject the new signals that are considered as outliers with large residuals. In consequence, adaptive parameters are chosen based on the covariance of the residuals. Residuals greater than their estimated standard deviation are not considered reliable. Numerous simulation results have conducted to choose the following parameters

$$c = \left(Jh_kP_{k|k-1}Jh_k^T + R\right)^{1/2}$$
$$a = c/2.$$

As the covariance increases due to few received signals, the proposed robust EKF does not reject new received signals when position uncertainty is large. Conversely, the misestimated pseudoranges are rejected when the position uncertainty is small.

III. Simulations

A. Simulation scenario

The proposed simulations consider a simplified 3D environment providing signals received at a given location in LOS or after one reflection. Simplifying hypotheses have been defined as follows

- The satellites are fixed, which is equivalent to consider that their ephemeris and their time of emission (information included in the GNSS signals) are known.
- The building are represented by blocks with flat surfaces.
- Only one signal can be received for each satellite (if a path exists between the satellite and receiver). Additional multipath signals that can be observed in practical situations are included in the noise.
- If a LOS signal exists, it is the one received by the GNSS receiver.
- This study only considers multipath signals obtained after a single reflection. This hypothesis is coherent with the results presented in [2] which show that multipath with only one reflection are generally the most powerful.

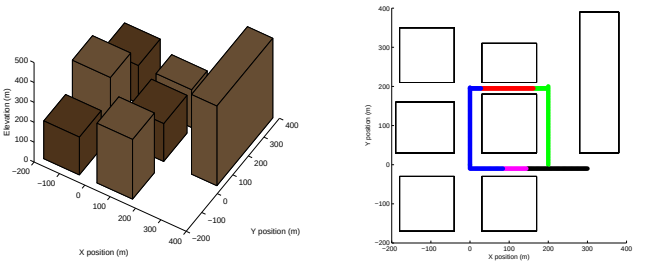

(a) 3D simplified environment used for the simulations.

(b) Trajectory simulated inside the city.

Fig. 3. Simulation scenario

A realistic trajectory of 900 m simulated inside the city is depicted in Fig. 3(b). The simulation has been generated in 3D even if only the 2D views have been represented (with transparent buildings) for clarity. The green part of the trajectory has been travelled first. In this first scenario, five satellites are available. However, three of them are in LOS during the first part of this trajectory whereas only two LOS signal have been received during the second part of this trajectory. The second part of the trajectory (in red) is the more constraint area with only one visible satellite. Five satellites are visible in the blue part of the trajectory, but with only two of them in LOS. These two satellites are the only ones visible during all the blue area, and unfortunately they have a bad DOP. At the beginning of the magenta area, a new signal appears. However, this signal is a multipath signal. We will see below that this signal can affect significantly the position estimation. Finally, in the black part of the trajectory, lots of satellites are visible again, with three of them in LOS.

B. Results

We first compare positioning results obtained with a classical EKF and the proposed 3D AEKF in our constraint envi-

ronment. Note that there is no noise affecting measurements in this simulation. Fig. 4 shows that the trilateration EKF is completely lost because of the large number of multipath received during all the trajectory. On the contrary, the 3D AEKF provides good results.

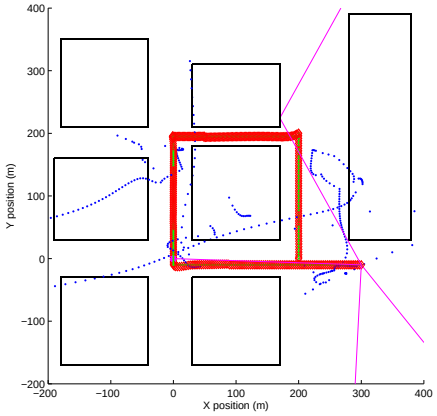

Fig. 4. Positioning results without additive noise. In green dot: real position. In blue dot: the trilateration EKF solution. In red diamond: the 3D AEKF solution. In magenta: the last received signals.

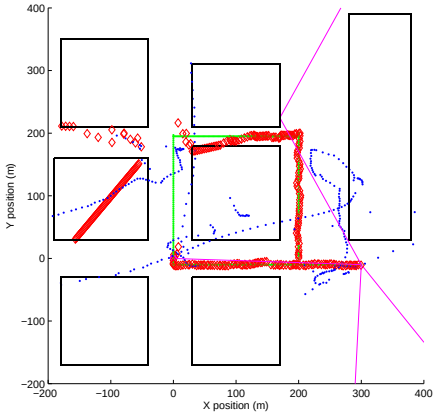

Fig. 5. Positioning result for an additive Gaussian noise with standard deviation $\sigma = 3m$. In green dot: real position. In blue dot: the trilateration EKF solution. In red diamond: the 3D AEKF solution. In magenta: the last received signals.

The second set of simulations compares the two methods in presence of an additive white Gaussian measurement noise with standard deviation $\sigma = 3m$ affecting the measured pseudoranges. Fig. 5 shows that the 3D AEKF begins to diverge during the red area (defined in Fig. 3(b)). This divergence is due to the lack of visible satellites. When the vehicle reaches the blue area, the local multipath environment varies too fast, producing aberrant position estimates. When the predicted position is in a building, the 3D AEKF becomes blind and therefore cannot correct the state vector until it leaves the building. However, as soon as the predicted position is outdoor, the proposed filter is able to converge to the correct position. Fig. 6 shows that the 3D AEKF always keeps its integrity even when the receiver is inside the building (blind area). The error associated with the 3D AEKF is generally lower than that obtained with the EKF except in the blind area. The errors on the pseudorange estimations are represented for two satellites in Fig. 7. Fig. 7(a) shows the case of a satellite that is always visible, and always in LOS. Conversely, the second satellite in Fig. 7(b) is almost always in NLOS when it is visible.

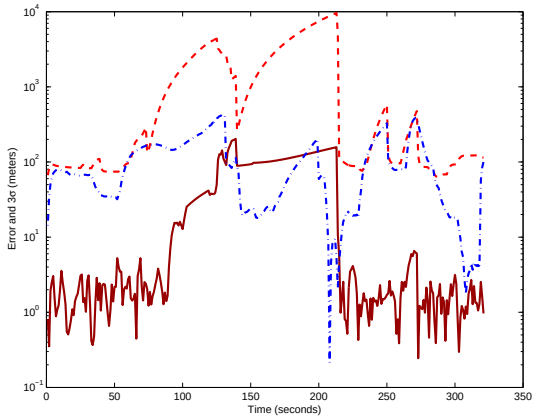

Fig. 6. Results for an additive Gaussian noise with standard deviation $\sigma = 3m$. In red: 3σ value at each time for the 3D AEKF. In blue: trilateration EKF position error. In dark red: 3D AEKF position error.

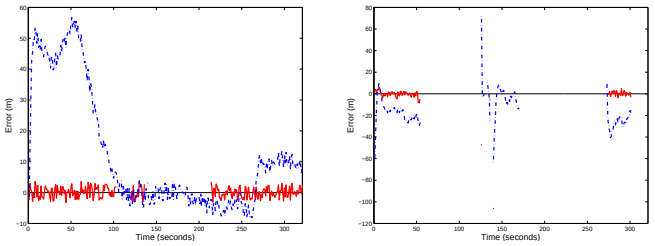

(a) Satellite 1 (b) Satellite 2

Fig. 7. Errors on the pseudorange estimations, for an additive Gaussian noise with standard deviation $\sigma = 3m$. In blue dashdot: the trilateration EKF. In red line: the 3D AEKF.

The same simulation is conducted with robust trilateration EKF and robust 3D AEKF. Fig. 8 shows that the robust trilateration EKF is able to give a good positioning solution when enough satellites are visible in LOS, i.e., at the beginning and at the end of the trajectory. Conversely, the robust trilateration EKF is lost when the NLOS dominate. The estimated position is also wrong in the magenta area (as defined in Fig. 3(b)). The use of all available information makes the robust 3D AEKF capable to quickly find the right position at the exit of the red area.

Fig. 9 shows small positioning errors for the robust 3D AEKF compared with the errors obtained with the robust trilateration EKF. In Fig. 10(a), we can see that the errors on the pseudorange estimations for satellite 1 are lower than the noise power for the robust 3D AEKF, which is not the case for the robust trilateration EKF. Fig. 10(b) shows that the 3D ANF method allows the pseudorange resulting from a NLOS satellite to be estimated correctly. The estimations are

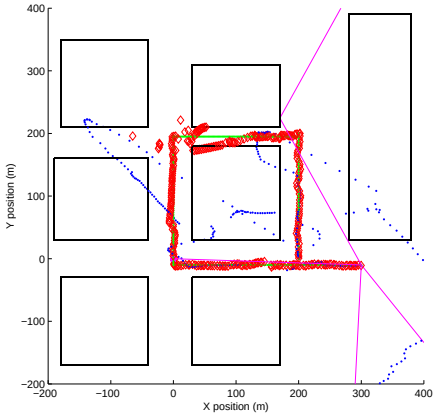

Fig. 8. Results for an additive Gaussian noise with standard deviation $\sigma = 3m$. In green dot: real position. In blue dot: the robust trilateration EKF solution. In red diamond: the robust 3D AEKF solution. In magenta: the last received signals.

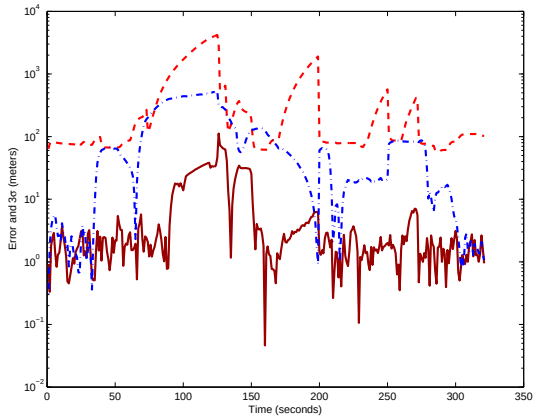

Fig. 9. Results for an additive Gaussian noise with standard deviation $\sigma = 3m$. In red: 3σ value at each time for the robust 3D AEKF. In blue: robust trilateration EKF position error. In dark red: robust 3D AEKF position error.

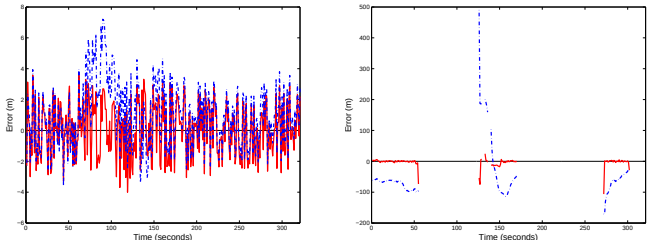

(a) Satellite 1 (b) Satellite 2

Fig. 10. Errors on the pseudorange estimations, for an additive Gaussian noise with standard deviation $\sigma = 3m$. In blue dashdot: robust trilateration EKF. In red line: robust 3D AEKF.

less accurate only at the beginning and at the end of a period during which the satellite is in view. However this inacurracy is mitigated by the robust part of the filter.

IV. Conclusion

This paper has proposed a new approach for GNSS navigation in critical NLOS environments. A tight integration of a 3D model of the environment with an extended Kalman filter allows NLOS signals to be used constructively. A robust version of the resulting navigation algorithm has also been investigated to use all the available information, even the less reliable measurements. Simulation results showed that the proposed robust 3D AEKF outperforms a classical robust EKF. These results are currently under validation using a more realistic model of the environment and real data. In these conditions, the inaccuracy of the model can be considered as an additive noise affecting the predicted measurements.

Acknowledgment

This work was supported by DGA (the French Defense Agency) and Thales Alenia Space, Toulouse, France.

References

[1] E. Kaplan and C. H. (Editors), *Understanding GPS: Principles and Applications*. 2nd Edition, Artech House, 2006.

[2] R. Ercek, P. De Doncker, and F. Grenez, "NLOS-multipath effects on pseudo-range estimation in urban canyons for GNSS applications," in *Proc. EuCAP-2006*, Nice, France, Nov. 2006, pp. 1–6.

[3] A. Van Dierendonck, "Theory and performance of narrow correlator spacing in a GPS receiver," *Navigation, J. Inst. Nav.*, vol. 39, no. 3, pp. 265–283, Fall 1992.

[4] M. Braasch, "Performance comparison of multipath mitigating receiver architectures," in *Proc. IEEE Aerosp. Conf.*, vol. 3, Big Sky, MT, 2001, pp. 1309–1315.

[5] M. Sahmoudi and M. Amin, "Fast iterative maximum-likelihood algorithm (FIMLA) for multipath mitigation in next generation of GNSS receivers," *IEEE Trans. Wireless Com.*, vol. 11, no. 7, pp. 4362–4374, Nov. 2008.

[6] P. D. Groves, "Shadow Matching: A new GNSS positioning technique for urban canyons," *J. Roy. Inst. Nav.*, vol. 64, pp. 417–430, 2011.

[7] D. Gustafson, J. Elwell, and J. Soltz, "Innovative indoor geolocation using RF multipath diversity," in *Proc. IEEE/ION Pos. Loc. Nav. Symp.*, San Diego, CA, April 2006, pp. 904–912.

[8] A. Soloviev and F. van Graas, "Utilizing multipath reflections in deeply integrated GPS/INS architecture for navigation in urban environments," in *Proc. IEEE/ION Pos. Loc. Nav. Symp.*, Monterey, CA, May 2008, pp. 383–393.

[9] A. Soloviev and F. V. Graas, "Use of deeply integrated GPS/INS architecture and laser scanners for the identification of multipath reflections in urban environments," *IEEE J. Sel. Topics Signal Process.*, vol. 3, no. 5, pp. 786–797, Oct. 2009.

[10] J. Bradbury, "Prediction of urban GNSS availability and signal degradation using virtual reality city models," in *Proc. ION GNSS Int. Tech. Meeting of the Sat. Div.*, Fort Worth, TX, Sept. 2007, pp. 2696–2706.

[11] K. D. Rao, M. N. S. Swamy, and E. I. Plotkin, "GPS navigation with increased immunity to modeling errors," *IEEE Trans. Aerosp. Electron. Syst.*, vol. 40, no. 1, pp. 2–11, Jan. 2004.

[12] A. Giremus, J.-Y. Tourneret, and V. Calmettes, "A particle filtering approach for joint detection/estimation of multipath effects on GPS measurements," *IEEE Trans. Signal Process.*, vol. 55, no. 4, pp. 1275–1285, April 2007.

[13] R. Ramlall, J. Streter, and J. F. Schnecker, "Three satellite navigation in an urban canyon using chip-scale atomic clock," in *Proc. ION GNSS Int. Tech. Meeting of the Sat. Div.*, Portland, OR, Sept. 2010, pp. 2937–.

[14] Y. Gao, "A new algorithm of receiver autonomous integrity monitoring (RAIM) for GPS navigation," in *Proc. ION GPS 1991*, Albuquerque, NM, 1991, pp. 887–896.